ELSEVIER

Fusion Engineering and Design 46 (1999) 1–9

Fusion Engineering and Design

www.elsevier.com/locate/fusengdes

Monte Carlo analysis of helium production in the ITER shielding blanket module

Satoshi Sato [a,*], Hiromasa Iida [b], Romano Plenteda [b], Robert T. Santoro [b]

[a] *Department of Fusion Engineering Research, Naka Fusion Research Establishment, Japan Atomic Energy Research Institute, Naka-machi, Naka-gun, Ibaraki-ken 311-0193, Japan*

[b] *ITER Garching Joint Working Site, Garching, Germany*

Received 29 July 1998; received in revised form 19 November 1998; accepted 1 February 1999

Abstract

In order to examine the shielding performances of the inboard blanket module in the International Thermonuclear Experimental Reactor (ITER), shielding calculations have been carried out using a three-dimensional Monte Carlo method. The impact of radiation streaming through the front access holes and gaps between adjacent blanket modules on the helium gas production in the branch pipe weld locations and back plate have been estimated. The three-dimensional model represents an 18° sector of the overall torus region and includes the vacuum vessel, inboard blanket and back plate, plasma region, and outboard reflecting medium. And it includes the 1 m high inboard mid-plane module and the 20 mm wide gaps between adjacent modules. From the calculated results for the reference design, it has been found that the helium production at the plug of the branch pipe is four to five times higher than the design goal of 1 appm for a neutron fluence of 0.9 MW a m^{-2} at the inboard mid-plane first wall. Also, it has been found that the helium production at the back plate behind the horizontal gap is about three times higher than the design goal. In the reference design, the stainless steel (SS):H_2O composition in the blanket module is 80:20%. Shielding calculations also have been carried out for the SS:H_2O composition of 70:30, 60:40, 50:50 and 40:60%. From the evaluated results for their design, it has been found that the dependence of helium production on the SS:H_2O composition in the blanket module is small at the branch pipe. Altering the steel–water ratio to reduce the amount of steel and increasing the thickness by >170 mm will reduce helium production to satisfy the design goal and not have a significant impact on weight limitations imposed by remote maintenance handling limitations. Also based on the calculated results, about 200 mm thick shields such as a key structure in the vertical gap are suggested to be installed in the horizontal gap as well to reduce the helium production at the back plate and to satisfy the design goal.

Keywords: ITER; Blanket module; Shielding calculations; Three-dimensional Monte Carlo method; Helium gas production; Radiation streaming

* Corresponding author. Tel.: +81-29-2707-583; fax: +81-29-2707-539.
E-mail address: sato@naka.jaeri.go.jp (S. Sato)

PII: S0920-3796(99)00006-X

1. Introduction

Three-dimensional Monte Carlo calculations have been carried out to estimate the shielding performance of the inboard blanket module proposed for use in the International Thermonuclear Experimental Reactor (ITER) Basic Performance Phase [1]. This study was performed to estimate the impact of radiation streaming through the front access holes in a blanket module and gaps between adjacent blanket modules on the helium gas production in the cooling water branch pipe weld locations and back plate. According to the current ITER design, the branch pipe access holes are bored through the face of the blanket. Plugs are installed at the boundary between the front access hole and branch pipe. The plugs, which are made of stainless-steel and serve as a pressure boundary, are to be cut and rewelded during a replacement of the blanket module. In addition to the plugs, the branch pipes near the back plate are also to be cut and rewelded during the module replacement.

The helium production in the plugs, branch pipes and back plate have been a critical concern from the viewpoint of rewelding. It is assumed here that rewelding of stainless-steel can be accomplished if the helium production within scheduled operation cycles is <1 appm which is a target goal for guiding shield design. Rewelding at higher helium concentrations may be possible depending on the welding procedure that is used.

Adjacent blanket modules are separated by 20 mm wide gaps in the poloidal (vertical) and toroidal (horizontal) directions. Field weld locations in the back plate are continuous in the vertical direction but are ~ 80 mm away from the vertical gap in the shadow of the module so that the weld seams are hidden by the module and the 14 MeV neutrons streaming do not pass directly through the vertical gaps to the welds. However, since 14 MeV neutrons streaming through the horizontal gaps see the welds because of the continuous vertical extent of the gaps, it is expected that the helium production is enhanced.

The radiation streaming impact has been investigated for various types of gaps and ducts [2–13]. However, these previously reported studies did not investigate the helium production in the cooling water branch pipe with the front access hole. The helium production in the back plate and the vacuum vessel has been calculated taking into account the radiation streaming through the gap in the vertical direction by El-Guebaly et al. [11] and Sato et al. [13]. These papers, however, did not investigate the radiation streaming impact through both gaps in the vertical and horizontal directions. In the present paper, the helium production in the blanket was investigated taking into account the radiation streaming impact through the front access hole and the gaps in the vertical and horizontal directions based on the current ITER shield blanket design.

The calculations summarized here were performed using the Monte Carlo Code MCNP [14] with transport cross-sections from the Fusion Evaluated Nuclear Data Library (FENDL) [15].

2. Geometry description

The three-dimensional calculation model is shown in Figs. 1 and 2. Cross sectional views are shown in Figs. 3 and 4. The model represents an

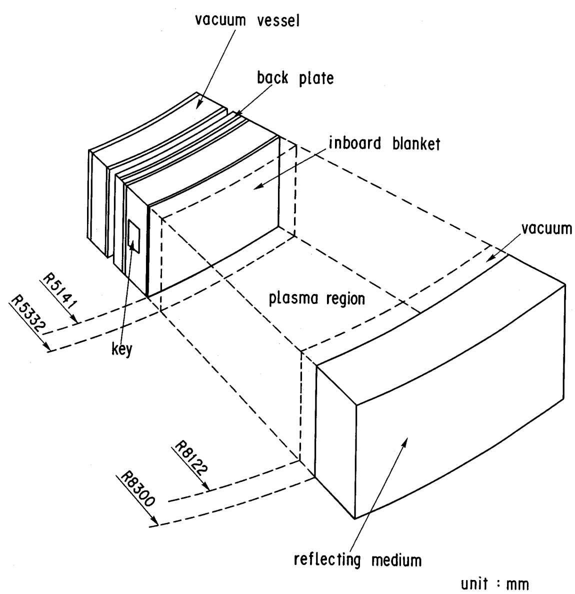

Fig. 1. View of the calculation model.

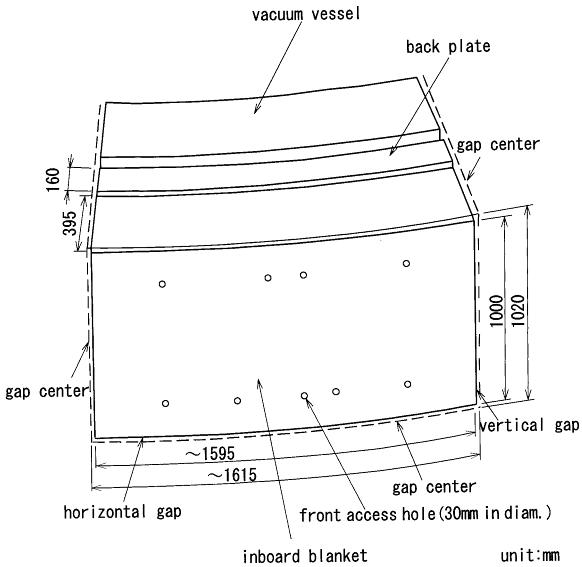

Fig. 2. Front view of the calculation model of the inboard blanket and vacuum vessel.

18° sector of the overall torus region and includes the vacuum vessel, inboard blanket and back plate, plasma region, and an outboard reflecting medium. The inner and outer major radii of the plasma are 5332 and 8122 mm, respectively. The calculational model includes the 1 m high inboard mid-plane module and the 20 mm wide gaps between adjacent modules. Reflective boundary conditions were imposed at the center of the poloidal and toroidal gaps. A reflecting medium having the same composition as the shielding

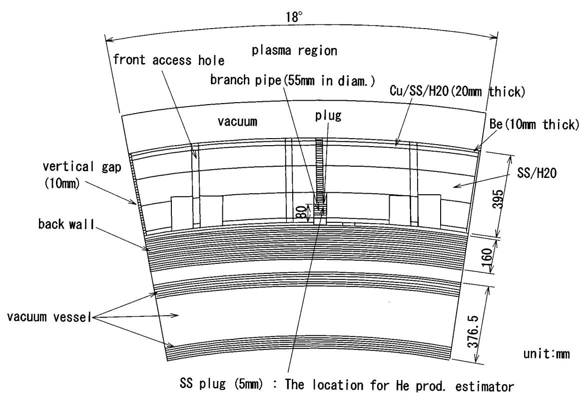

Fig. 3. Cross-sectional view of the calculation model.

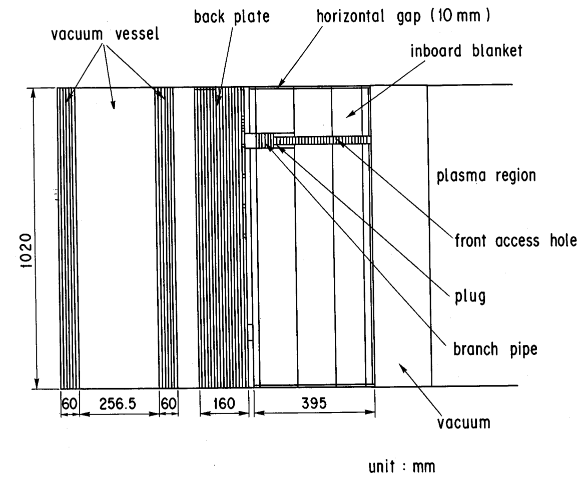

Fig. 4. Cross-sectional view of the calculation model.

blanket is placed at 8300 mm from the torus axis (center axis in the torus) to simulate the outboard module to assure the realistic neutron spectrum incident on the inboard blanket.

The inboard blanket module is 395 mm thick and contains nine 30 mm diameter front access holes. The module is attached to a 160 mm thick double walled back plate. The module is composed of the first wall and the shield block. The first wall faces the plasma, and is required to be designed to withstand the high heat flux from the plasma. The first wall assembly consists of a 10 mm thick Be layer (100%) followed by a 20 mm thick Cu:H_2O:stainless Steel (SS) heat sink (74.3% Cu; 17.8%H_2O; 7.9% SS) where these materials were homogenized in the calculations. Two 55 mm diameter water filled branch pipes having a total length of 96 mm were also modeled with 80 mm of the pipe in the module and the remaining 16 mm in the space between the module and the back plate. A 5 mm thick stainless-steel plug that is attached to the front of the branch pipe was used as the location for estimating the helium production. Except for the first wall, the front access holes and the branch pipes, the inboard blanket module composition were treated to be a homogenized mixture of 80% SS;20% H_2O. The back plate is comprised of a 50 mm thick inner wall (100% SS), a 40-mm-thick manifold (100% H_2O) and a 70 mm thick outer wall (100% SS).

The inboard vacuum vessel consists of a 60 mm thick inner wall (100% SS), 255 mm thick shield layer (80% SS:20% H_2O) and a 60 mm thick outer wall (100% SS).

The outboard blanket was represented by a homogenized layer of 80% SS:20% H_2O to reflect the plasma neutrons.

3. Stainless-steel composition and evaluation method

The helium production in stainless-steel occurs principally from fast neutron reactions with the Ni, Fe and Cr component in the steel. However, ^{10}B, which is an isotope of a trace element of boron in stainless-steel, has a very large (n, α) cross-section (~ 4000 *b* for thermal neutrons and an $E^{-1/2}$ dependence in the epithermal region). Even though the trace amount of boron is small, the $^{10}B(n, \alpha)$reaction with low energy neutrons results in a large amount of helium production. The helium production in water filled pipes is further enhanced due to increase of the thermal neutron in the water cooling channels adjacent to the weld locations.

ITER grade stainless-steel (SS316L(N)-IG) originally recommended as the structural material for the shielding blanket assembly is specified to contain 20 parts per million by weight (wppm) B. Neutronics calculations [16] have, however, suggested that reduction of the boron concentration to ≤ 10 wppm decreases the helium production rate by up to a factor of two. In this study, SS316L(N)-IG with 10 wppm B is used as the stainless steel material for the evaluation of the helium production.

Helium production rate has been evaluated by using the track length estimate of cell flux (F4) and the weight window technique which is a space-energy-dependent splitting and Russian roulette variance reduction procedure [14].

4. Neutron wall loading

Source neutrons in the plasma region shown in Fig. 1 were sampled from an isotropic neutron distribution having a Muir velocity Gaussian fusion energy spectrum [14] and normalized to an average 14 MeV neutron current of 4.439×10^{13} cm^{-2} s^{-1} which corresponds to an average neutron wall loading of 1 MW m^{-2} at the first wall surfaces of the inboard and the outboard blankets. The Muir velocity Gaussian fusion energy spectrum is expressed by the following formula;

$$p(E) = C \times e^{-(\sqrt{E}-\sqrt{b}/a)^2}$$

where a is the width in MeV$^{1/2}$, and b is the energy in MeV corresponding to the average speed [14].

The average 14 MeV neutron currents at these surfaces are 3.3 and 5.2×10^{13} cm^{-2} s^{-1}, respectively, and correspond to average neutron wall loadings of 0.75 and 1.2 MW m^{-2}, respectively. In the calculations reported by Valenza et. al. [17], neutron wall loadings at the inboard and the outboard mid-plane of 0.9 and 1.25 MW m^{-2}, respectively, were reported. Since the neutron wall loadings at the lower and upper poloidal regions in the actual ITER geometry are small compared with those at the mid-plane, the average neutron wall loadings at the inboard and outboard region in the model used in this study are expected to be lower compared with 0.9 and 1.25 MW m^{-2}, respectively. Therefore, the neutron wall loadings and nuclear responses in the inboard blanket module were finally normalized to a neutron wall loading of 0.9 MW m^{-2}, which was an actual condition for the inboard mid-plane first wall.

5. Helium production

5.1. Branch pipe

Helium production distributions which were normalized to a neutron fluence of 0.9 MW a m^{-2} at the inboard mid-plane first wall, in the front access hole and the branch pipe are shown in Fig. 5. Also shown in the figure are the helium production distributions for the case with no front access hole, and for the case with no water in the branch pipe. The helium production distribution for the case when ordinary SS316L(N)-IG (20 wppm Boron) is used as the structural material is also plotted. The number of history, statistical errors for the estimation of the helium production at the plug and computation time are also shown in the figure.

For the reference design [see Ref. [1] which used SS316L(N)-IG (10 wppm Boron)], the helium production at the plug which corresponds to the location of rewelding is four to five times higher than the design goal of 1 appm. In the branch pipe, the helium in the stainless-steel is produced by both fast and thermal neutron reactions since the fraction of thermal neutrons is enhanced by the water in the branch pipe. The helium production at a location about 23 mm away from the plug is about 7 appm. It is also observed that the helium production at the plug is 3–4 appm and will not meet the design goal even if there were no front access holes. The helium production at the plug for the case of the ordinary SS316L(N)-IG (20 wppm Boron) is about 1.7 times higher than that for the reference with the SS316L(N)-IG composition with 10 wppm Boron.

The case with no water in the pipe is shown for comparison. Although the shielding effectiveness for fast neutrons in the case without the water in the branch pipe is less than that for the case with water, helium production for the case without water is much smaller because there is less thermal neutron flux in the pipe. In the case of no water in the branch pipe, which infers a hypothetical design that fully eliminates thermal neutrons by the use of a neutron absorbing material, e.g. Cd, the helium production in the plug can be reduced to about 60% of the helium production in the reference design. The helium production in the plug is about 2 appm even when there is no water in the branch pipe. Shown in Fig. 6 are the helium production distributions for the cases where the access hole diameters are increased to 40, 50, 60 and 80 mm. For these cases, the helium productions in the branch pipe are 1.15, 1.3, 1.7 and 2.1 times higher, respectively, than those for the case when the pipe diameter is 30 mm.

Helium production distributions for the cases when the inboard blanket thickness are increased by 100 and 170 mm, i.e. the total thickness equals 495 and 565 mm, respectively, are shown in Fig. 7. Based on these data, it is found that if the thickness of the inboard blanket module is increased by more than 170 mm, the helium production design goal at the plug of the branch pipe can be achieved.

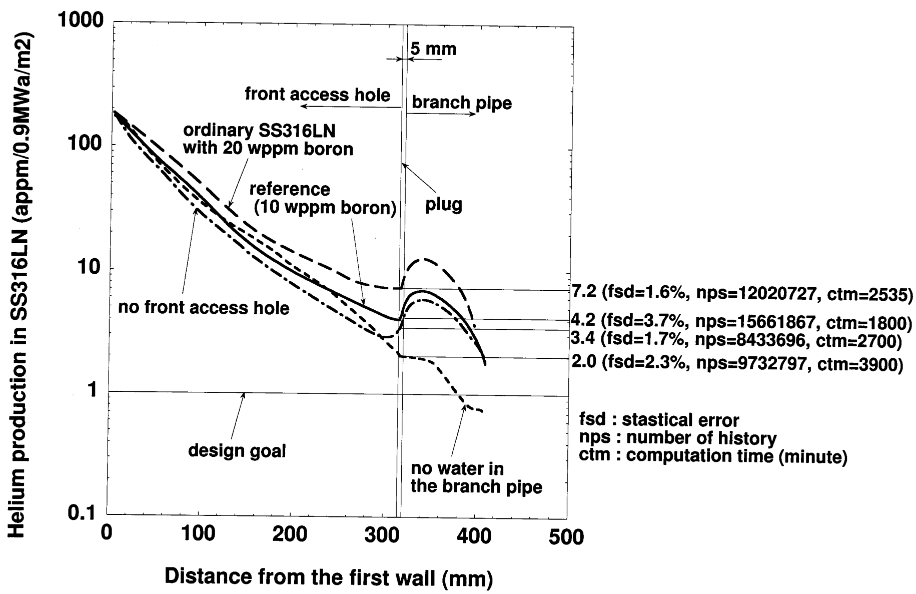

Fig. 5. Helium production in the front access hole and branch pipe.

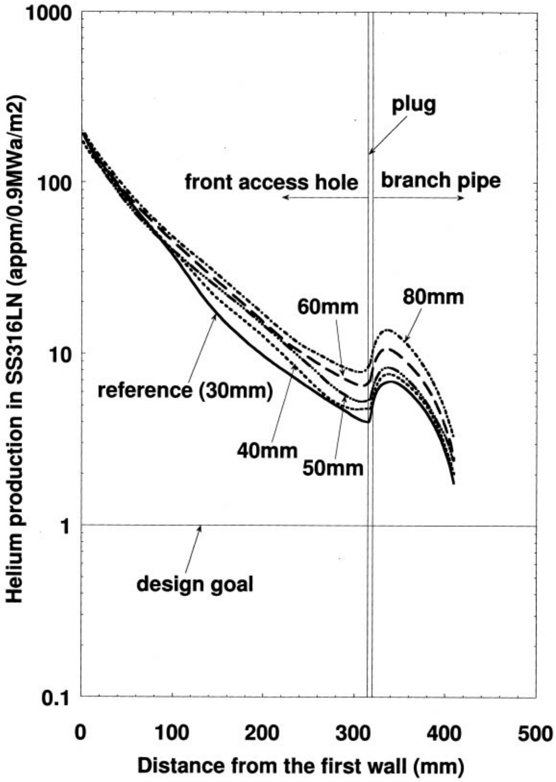

Fig. 6. Helium production distribution in the front access hole and branch pipe for front access holes with diameters between 30 and 80 mm.

Helium production distributions are shown in Fig. 8 for the case of the 565 mm thick blanket module, comparing SS:H_2O compositions of 80:20, 70:30, 60:40, 50:50 and 40:60%. It is found that a 70:30 composition is optimum for reducing the helium production at the plug of the branch pipe. It is also observed that helium production at the plug in the case of 40:60 mixture is about 1.6 times higher than for the 80:20 composition, but the design goal can still be met. If the blanket module thickness is increased by >170 mm and the SS:H_2O mixture is changed to a 40:60 ratio, helium production can be reduced maintaining the overall weight of the module identical to that for the reference case. When the blanket module thickness is increased by 170 mm, it might be required that the vacuum vessel thickness is reduced by 170 mm from the severe restriction of the space point of view.

Helium production distributions are shown in Fig. 9 for the case of a 565 mm thick blanket module (SS:H_2O compositions of 70:30) with a front access hole of 40 mm diameter. It is found that the helium production at the plug is about 1.1 times higher than for the case of a 30 mm diameter access hole and satisfies the design goal.

5.2. Back plate

Helium production distributions in the 20 mm wide horizontal gap between the adjacent blanket modules are shown in Fig. 10. Tally cells which were the detector for the helium production estimation were installed at 0.3–1.8° from the center of the vertical gap which corresponds to distances between 26 and 154 mm from the vertical gap center and covered the welding locations at the back plate.

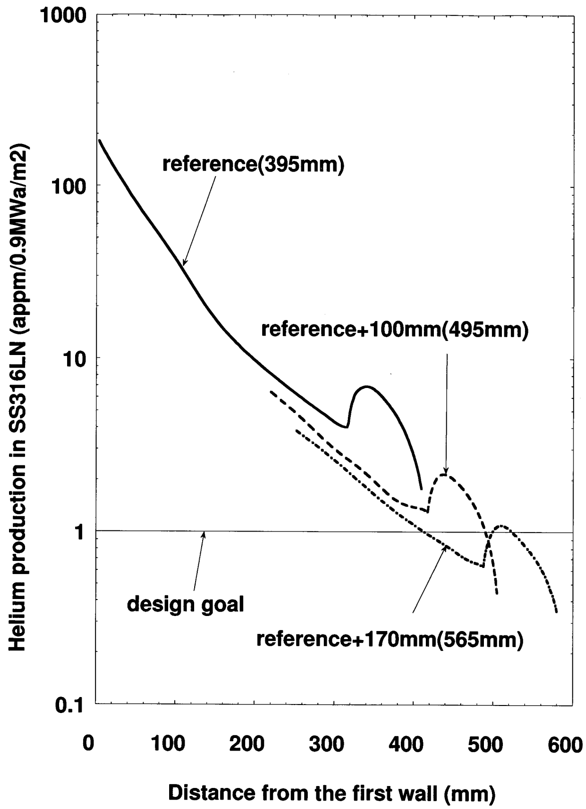

Fig. 7. Helium production in the front access hole and branch pipe for module thickness between 395 and 565 mm.

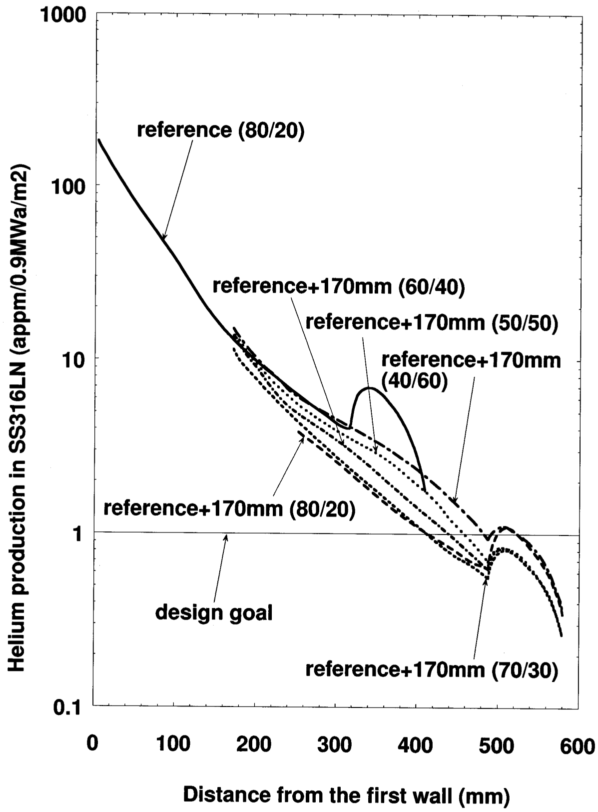

Fig. 8. Helium production distributions in the front access hole and branch pipe as a function of stainless steel (SS):H_2O composition.

Shown in Fig. 10 is the helium production distribution in the reference design along with those for the cases when 52, 102, 202 and 302 mm thick shields (80% SS:20% H_2O) are installed at the end of the horizontal gap in front of the back plate at locations where welding is required. The helium production at the inner surface of the inner wall of the back plate at 100 mm from the horizontal gap center in the reference design is shown as a solid circle.

In the case of the reference design, the helium production at the inner surface of the inner wall is about three times higher than the design goal while the helium production at the back of the inner wall satisfies the design goal. At a location 100 mm away from the horizontal gap center, the helium production is reduced by about one order of magnitude and fully satisfies the design goal. If a 202 mm thick shield can be installed in the horizontal gap, helium production can be within the design goal. In the actual design, an $\sim$190 mm thick key is installed in the vertical gap and fills the role of a shield. There is, however, no key in the horizontal gap in the current design.

The helium production distributions along the toroidal direction at the inner surface of the inner wall are shown in Fig. 11 for the reference design. The horizontal axis corresponds to the distance from the center of the vertical gap. The solid line is the helium production distribution behind the horizontal gap and the dotted line shows the helium production at a distance of 100 mm from the horizontal gap center. It is found that the helium production distribution is almost constant behind the horizontal gap and it reduces gradually

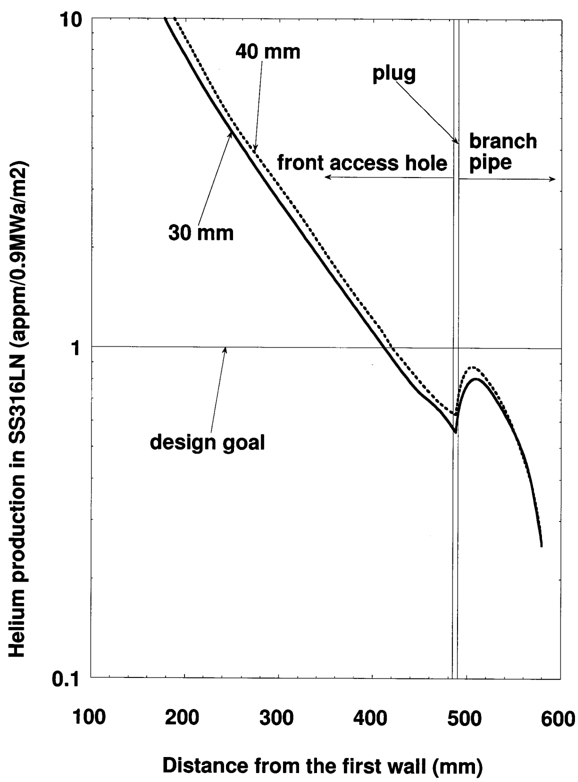

Fig. 9. Helium production distribution in the front access hole and branch pipe for the 565 mm thick module for front access holes of 30 and 40 mm diameter.

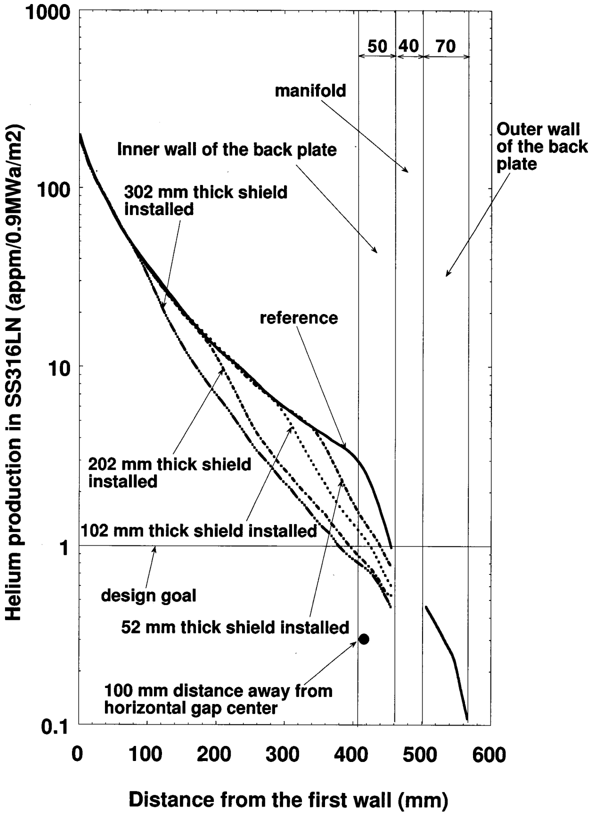

Fig. 10. Helium production in the horizontal gap and back plate behind the gap.

at locations 100 mm distance from the horizontal gap center.

6. Conclusions

Through the three-dimensional Monte Carlo shielding analyses of the ITER shielding blanket module, the following results were obtained.

(1) The helium production at the plug of the branch pipe is four to five times higher than the design goal of 1 appm for a neutron fluence of 0.9 MW a m^{-2} at the inboard mid-plane first wall.

(2) In the case when there is no water in the branch pipe, the helium production at the plug is reduced to about 2 appm and is still above the design specification.

(3) The dependence of helium production on the SS:H_2O composition in the blanket module is small at the branch pipe. Altering the steel–water ratio to reduce the amount of steel and increasing the thickness by >170 mm will reduce helium production to satisfy the design goal and not have a significant impact on weight limitations imposed by remote maintenance handling limitations.

(4) The helium production at the back plate at ~ 100 mm distance from the horizontal gap is one order of magnitude lower than that behind the horizontal gap and within the design goal.

(5) The helium production at the back plate behind the horizontal gap is about three times higher than the design goal.

(6) About 200 mm thick shield material such as the key in the vertical gap is suggested to be installed in the horizontal gap as well to reduce the helium production at the back plate and to satisfy the design goal.

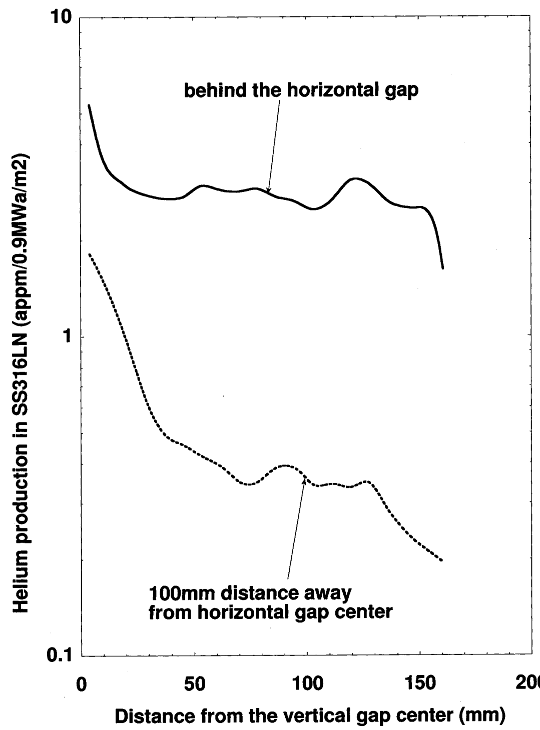

Fig. 11. Helium production distributions in the back plate.

Acknowledgements

This work was performed as part of the design study of ITER conducted by the ITER Joint Central Team Garching Site which is under the leadership of Dr R. Parker. The authors wish to thank him and the team members. Also, the authors would like to express their sincere appreciation to Drs M. Ohta, S. Matsuda, H. Takatsu and Y. Ohara for their continuous guidance and encouragement.

References

[1] F. Elio, et al., Progress in the ITER Blanket Design, Proc. 17th Symp. on Fusion Eng., San Diego, October, 1997.
[2] W.T. Urban, et al., Engineering test facility vacuum pumping duct shield analysis, Nucl. Technol./Fusion 2 (1982) 261–271.
[3] Y. Seki, et al., Radiation streaming calculations for INTOR-J, Nucl. Technol./Fusion 2 (1982) 272–285.
[4] Y. Seki, et al., Radiation shielding considerations for the repair and maintenance of a swimming pool-type tokamak reactor, Nucl. Eng. Des./Fusion 1 (1984) 243–253.
[5] K. Ueki, et al., Analysis of 14 MeV neutron streaming through a narrow hole-duct using the Monte Carlo technique, Fusion Technol. 7 (1985) 90.
[6] K. Shin, et al., Semiempirical formula for energy-space distributions of streamed neutrons and gamma-rays in cylindrical ducts, J. Nucl. Sci. Technol. 25 (1988) 8.
[7] K. Shin, et al., A simple calculation method for 14 MeV neutron gap streaming, Fusion Eng. Des. 10 (1989) 115.
[8] S.A. Zimin, An analysis of radiation streaming through inhomogeneities in the fusion reactor blanket and shield, Fusion Technol. 17 (1990) 371.
[9] K. Maki, et al., Radiation shielding for superconductive toroidal field coils around the neutral beam injector duct in the ITER design, Fusion Eng. Des. 22 (1993) 427–434.
[10] S. Sato, et al., Evaluation of radiation streaming through the annular gaps around divertor cooling pipes in fusion experimental reactors, Proceedings of 8th International Conference on Radiation Shielding, Arlington, TX, USA, April 24–28, 1994, pp. 1039–1046.
[11] L.A. El-Guebaly, et al., Shielding analysis for ITER with impact of assembly gaps and design inhomogeneities, Proceedings of 8th International Conference on Radiation Shielding, Arlington, TX, USA, April 24–28, 1994, pp. 1047–1054.
[12] S. Sato, et al., Shielding analysis for toroidal field coils around exhaust duct in fusion experimental reactors, Fusion Technol. 30 (1996) 1076.
[13] S. Sato, et al., Streaming analysis of gap between blanket modules for fusion experimental reactor, Fusion Technol. 30 (1996) 1129.
[14] J.F. Briesmeister, MCNP 4A Monte Carlo N-Particle Transport Code System, Oak Ridge National Laboratory, RSICC Computer Code Collection, June, 1995.
[15] IAEA Specialist Meeting on the Fusion Evaluated Nuclear Data Library (FENDL), Vienna, Austria, May 1989; Summary Report edited by V. Goulo and published as IAEA Nuclear Data Section Report INDC (NDC)-223/GF, (1989).
[16] R.T. Santoro, Material Compositions for the Blanket, Vacuum Vessel, Cryostat, and Biological Shield, ITER Garching Joint Work Site, ITER Report Number NAG-38-24-06-97, 1997.
[17] D. Valenza, H. Iida, R.T. Santoro, Poloidal Distributions of the Neutron Wall Loading and Nuclear Heating in the ITER First Wall Using the 3-D Monte Carlo Code MCNP, ITER Garching Joint Work Site, ITER Report Number NAG-52-4-16-96, 1996.